



Combined UHV and ambient pressure studies of 1,3-butadiene adsorption and reaction on Pd(1 1 1) by GC, IRAS and XPS

Joaquin Silvestre-Albero ¹, Marta Borasio ¹, Günther Rupprechter ^{*}, Hans-Joachim Freund

Fritz-Haber-Institut, Faradayweg 4-6, 14195 Berlin, Germany

Received 3 February 2006; received in revised form 29 June 2006; accepted 29 June 2006

Abstract

The hydrogenation of 1,3-butadiene on Pd(1 1 1) at 300 K was studied at atmospheric pressure by infrared reflection absorption spectroscopy (IRAS) and gas chromatography (GC). Kinetic measurements showed 1-butene, *trans*-2-butene and *cis*-2-butene as primary products. Once 1,3-butadiene had been completely consumed, 1-butene was re-adsorbed on the surface producing *trans*-/*cis*-2-butene through isomerization and *n*-butane through hydrogenation. These results were corroborated by in situ IRAS spectroscopy. Post-reaction analysis by X-ray photoelectron spectroscopy (XPS) in the C1s region revealed a band at 284.2 eV, corresponding to adsorbed butadiene and/or carbonaceous deposits. Quantification of this peak revealed a total carbon coverage of 0.3 ML. Nevertheless, deactivation due to carbon deposition was a minor effect under our reaction conditions, as indicated by the kinetics of the subsequent butene hydrogenation reaction. Temperature-dependent XPS experiments after butadiene adsorption at 100 K indicated a high stability of the diene molecule with hardly any desorption and/or decomposition up to 500 K. Above this temperature, butadiene decomposed to carbon species that eventually dissolved in the Pd bulk above 700 K.

© 2006 Elsevier B.V. All rights reserved.

1. Introduction

The catalytic hydrogenation of 1,3-butadiene is an interesting process, both from an industrial and academic point of view. There are four reaction products (1-butene, *trans*/*cis*-2-butene and *n*-butane) and, consequently, regioselectivity is required to obtain the desired compound [1–4]. Previous studies have shown that Pd catalysts are highly active and highly selective towards butene formation while Pt catalysts mostly yield *n*-butane via complete hydrogenation [5]. Different adsorption modes of 1,3-butadiene, i.e. di- σ adsorption on Pt and di- π adsorption on Pd [6,7], were made responsible for the different catalytic behavior. How-

ever, the activity/selectivity of the title reaction do not only depend on the butadiene adsorption geometry. The adsorption energy and stability of the different intermediate products, and also of hydrogen, will affect surface coverage and eventually selectivity. Along these lines, Massardier et al. attributed the lower activity of platinum catalysts to a low hydrogen coverage [5], resulting from a low H₂ adsorption energy and sticking coefficient [8]. Additionally, the similar adsorption energy of 1,3-butadiene and butenes on Pt surfaces was used to explain the low selectivity towards butene formation on Pt, in contrast to Pd surfaces where the diene is more strongly adsorbed than the butenes (leading to higher butene selectivity) [9].

Previous studies on the stability (adsorption energy) of 1,3-butadiene on noble metal single crystals have shown a strong dependence both on the metal and the crystallographic surface orientation. Zhao and Koel reported a high stability of butadiene adsorbed on Pt(1 1 1) at 100 K towards desorption [10]. While at low coverage (0.06 L) no butadiene

^{*} Corresponding author. Permanent address: Institute of Materials Chemistry, Vienna University of Technology, Veterinärplatz 1, A-1210 Vienna, Austria. Tel.: +43 1 25077 3801; fax: +43 1 25077 3890.

E-mail address: rupp@imc.tuwien.ac.at (G. Rupprechter).

¹ These authors have equally contributed to the results.

desorption was observed, higher exposures (0.24 L) led to a single desorption peak at 130 K, due to multilayer desorption. Some H₂ desorption (370–585 K) together with surface carbon formation indicated a limited amount of butadiene decomposition. However, similar studies on H-precovered Pd(110) crystals showed desorption of both physisorbed and chemisorbed butadiene below 200 K [11].

In previous studies we have reported that the catalytic activity and selectivity in the 1,3-butadiene hydrogenation reaction on Pd catalysts depends both on the crystallographic orientation [12] and the Pd particle size [13]. Additionally, we have shown that the presence of CO traces can modify in a great extent the selectivity towards the intermediate hydrogenated products by reducing the surface hydrogen concentration. Besides catalytic activity and selectivity, another important aspect in these hydrogenation reactions is catalyst deactivation, both via strongly adsorbed surface species and/or via carbon deposits. In this sense, the formation of carbonaceous deposits under reaction conditions was proposed as being responsible for the increased selectivity of Pd catalysts after achieving steady state conditions in the 1,3-butadiene hydrogenation reaction [9]. However, despite the crucial role of carbonaceous deposits, to our knowledge there are no studies about the stability of butadiene on Pd surfaces or an analysis of the nature of the surface species present after the reaction, such as CH_x and/or C species. Therefore, the aim of the current work was to examine the hydrogenation of 1,3-butadiene at atmospheric pressure on Pd(111) by infrared reflection absorption spectroscopy (IRAS) and by on-line gas chromatography (GC). X-ray photoelectron spectroscopy (XPS) and low energy electron diffraction (LEED) were employed for pre- and post-reaction surface analysis. Finally, the adsorption and desorption of butadiene was studied in UHV by XPS, following the C1s and Pd3d signals. These results should provide a basis to address the role of carbonaceous species during selective butadiene hydrogenation.

2. Experimental section

The experiments were carried out in a UHV surface analysis chamber combined with a UHV-high-pressure reaction cell optimized for grazing incidence IRAS [14a]. The UHV section was equipped with LEED and XPS (Specs Phoibos 150 using Mg K α irradiation with a resolution of \sim 1 eV; electron analyzer at a constant pass energy of 20 eV). The Pd(111) single crystal was prepared by sequences of ion bombardment, oxidation and annealing as described in Ref. [14b]. The surface structure and cleanliness were confirmed by LEED and XPS, respectively, and were also indirectly examined by IRAS using CO as a probe molecule. Only for clean, well-annealed Pd(111) CO produces a perfect (2 \times 2)-3CO structure, which exhibits a characteristic vibrational spectrum with narrow peaks around 1895 cm⁻¹ and 2105 cm⁻¹ [14]. High purity gases, 1,3-butadiene (99+%; Aldrich) and H₂ (99.9999%; Linde),

were used. Butadiene exposures under UHV, as measured by an ionization gauge, were corrected by the gauge sensitivity factor of 4.

XPS experiments were performed in UHV after dosing butadiene at 100 K. The growth and desorption of butadiene were detected by following the C1s and Pd3d XP spectra. Quantitative XPS analysis of the surface carbon concentration was performed by using the (2 \times 2)-3CO saturation structure of CO on Pd(111) (coverage 0.75 ML) as reference (assuming identical sensitivity factors for CO, C and CH_x). Peak deconvolution was performed using the Levenberg–Marquardt method (standard non-linear least-squares algorithm), using a mix of Gaussian and Lorentzian shapes and a tail function.

In situ infrared spectroscopic studies during catalytic 1,3-butadiene hydrogenation were performed using a Bruker IFS66v/S FTIR spectrometer. Prior to the experiments, the clean model catalyst was transferred from UHV to the high-pressure cell (under UHV). The sample was then contacted with a butadiene/hydrogen (1:2) reaction mixture (10 mbar total pressure) at 300 K. IRAS spectra were acquired every 5 min using a spectral resolution of 4 cm⁻¹. The observed spectra are basically IR gas phase spectra. Vibrational signatures of surface species were not obtained.

Kinetic measurements of 1,3-butadiene hydrogenation were performed in a second UHV apparatus very similar to the one used for IRAS experiments but connected *on-line* to a gas-chromatograph [12,13]. Measurements were done at atmospheric pressure (reaction mixture: P_{1,3-butadiene}: 5 mbar; P_{H₂}: 10 mbar; Ar added up to 1 bar) in the temperature range 300–373 K in a recirculated batch mode. Reaction products were analyzed by on-line gas chromatography, using a HP-PLOT/Al₂O₃ (50 m \times 0.53 mm) capillary column and a flame ionization detector (FID). Retention times and sensitivity factors for the reactant and the products were calibrated using a number of different gas mixtures. Using Al₂O₃ films on NiAl(110) as “inert” catalysts the absence of background (wall) reactions under typical operating conditions was confirmed.

3. Results and discussion

3.1. Ambient pressure measurements

Fig. 1a shows GC kinetic measurements of 1,3-butadiene hydrogenation on Pd(111) at 300 K. As mentioned, the reaction is interesting due to the four different reaction products and due to the necessity of regioselectivity towards the desired product 1-butene. In the first minutes of the reaction 1,3-butadiene is hydrogenated to the three butenes (1-butene, *trans*-2-butene and *cis*-2-butene). Analysis of the yield to the different butenes at zero conversion indicated that the three butenes are primary products. There are also mechanistic studies by Wells and coworkers [15] using deuterated butadiene which suggested the primary character of the three butenes on Pd catalysts. It is

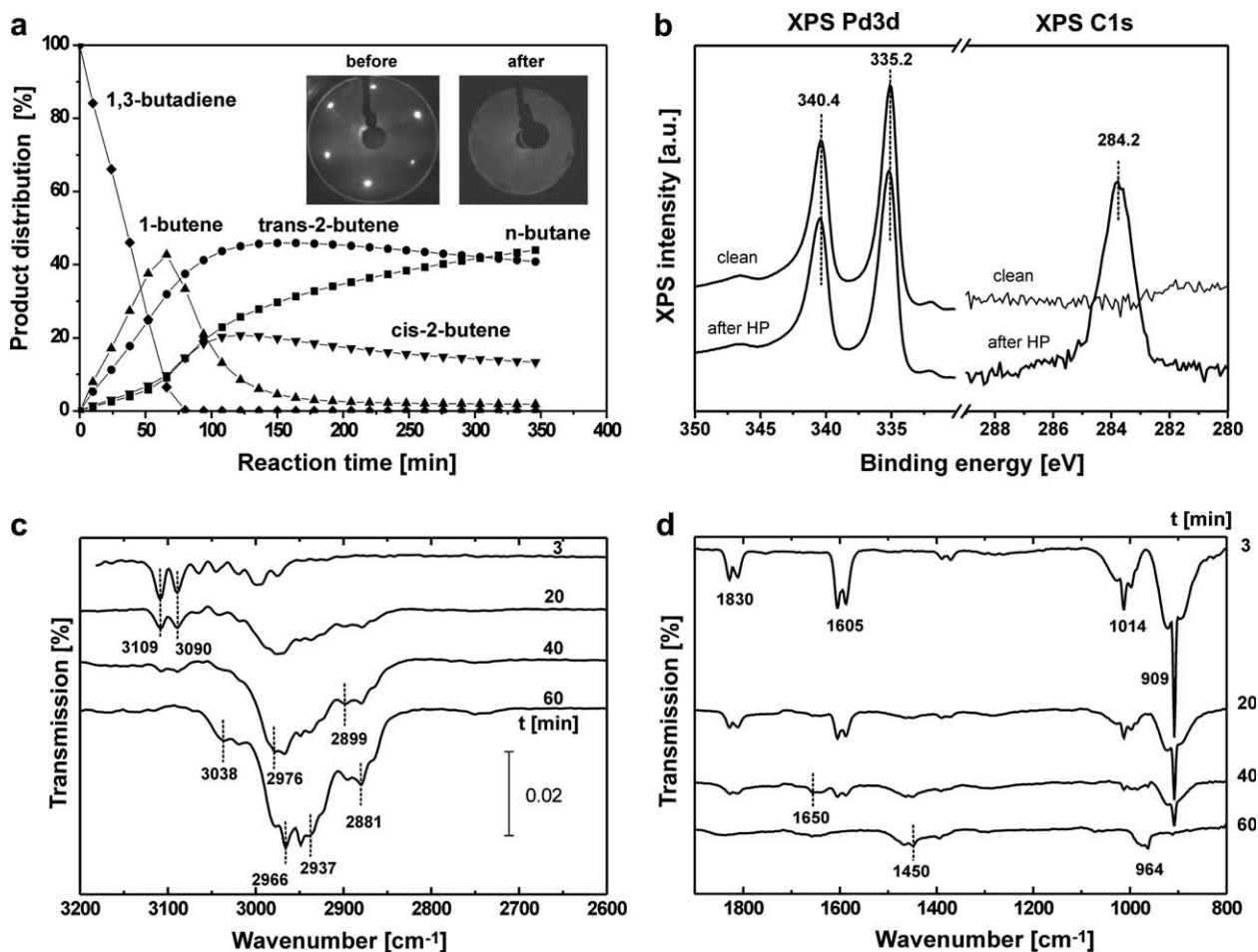


Fig. 1. (a) Product distribution versus reaction time for 1,3-butadiene hydrogenation on Pd(111) at 300 K ($P_{1,3\text{-butadiene}}$: 5 mbar; P_{H_2} : 10 mbar; Ar added up to 1 bar); (b) post-reaction XPS analysis in the Pd3d and C1s region (after 60 min high-pressure (HP) reaction); (c), (d) are IRAS measurements during the catalytic reaction at 300 K ($P_{1,3\text{-butadiene}}$: 3.3 mbar; P_{H_2} : 6.7 mbar) after 3 min, 20 min, 40 min and 60 min reaction time.

noteworthy that 1-butene, the thermodynamically least stable product, is the main product after the first hydrogenation step. Interestingly, there is also some *n*-butane formation after a few minutes, resulting from subsequent hydrogenation of adsorbed and/or re-adsorbed butenes even in the presence of butadiene. The re-adsorption and reaction of butenes is more pronounced after complete 1,3-butadiene consumption (~ 75 min). 1-Butene considerably re-adsorbs on the surface leading to two reaction processes, i.e. *n*-butane formation through hydrogenation and *trans/cis*-2-butene formation through isomerization. With decreasing 1-butene pressure (concentration), 2-butene re-adsorption and hydrogenation started.

Fig. 1a also shows pre- and post-reaction LEED images as inset. The clean Pd(111) crystal exhibited the typical hexagonal pattern while after 6 h reaction time the LEED pattern was diffuse. This is a clear indication of the presence of adsorbed surface species, most probably of adsorbed (disordered) butadiene together with carbonaceous species. It is interesting to note that the original LEED pattern could be recovered after a high temperature flash (900 K) which can be explained by desorption/decomposition of butadiene and by dissolution of the carbon species in the Pd bulk.

The selectivity of 1,3-butadiene hydrogenation is defined by the ratio of 1,2-H addition (yielding 1-butene) vs. 1,4-H addition (yielding 2-butene) to butadiene. Consequently, this process is in part governed by the geometry of the adsorbed molecule on the surface. Previous studies by near-edge X-ray absorption fine structure (NEXAFS) and high-resolution electron energy loss spectroscopy (HREELS) on Pd single crystals have shown that butadiene preferentially adsorbs via the two double bonds in a di- π configuration [7]. However, DFT calculations of butadiene adsorption on Pd(111) suggest the 1,2,3,4-tetra- σ adsorption state with a total adsorption energy of $-166 \text{ kJ} \cdot \text{mol}^{-1}$ [16]. In order to identify the nature of the surface species during the reaction we have performed IRAS measurements on the Pd(111) crystal under in situ reaction conditions. Unfortunately, only gas phase and no surface species could be observed in the spectra, probably due to the flat adsorption geometry of the different molecules on the surface. In fact, only those molecular vibrations that have a dipole component normal to the surface will contribute to the IRAS signal. An absence of surface signals was also reported in previous IRAS studies of butadiene hydrogenation on Pt(111) and Pt₃Sn(111) [17].

Adsorption studies of 1,3-butadiene on Pd(110) by HREELS and NEXAFS have also shown that the molecule adsorbs parallel on the surface [18].

Nevertheless, the reaction could be monitored by IR gas phase spectroscopy as shown in Fig. 1c,d. At the beginning of the reaction the IR spectra exhibited the characteristic bands of (pure) 1,3-butadiene in the gas phase (Fig. 1c,d; spectra after 3 min). The main bands are in the range 2976–3109 cm^{-1} , corresponding to a combination of symmetric and asymmetric νCH and νCH_2 in-plane stretching vibrations (Fig. 1c) and at 1830 cm^{-1} , 1605 cm^{-1} , 1014 cm^{-1} and 909 cm^{-1} , corresponding to $\text{C}=\text{CH}_2$ stretching, $\text{C}=\text{C}$ stretching, CH bending and CH_2 twisting and wagging vibrations, respectively (Fig. 1d). With reaction time, the characteristic bands of butadiene progressively decreased, while new bands appeared at 2976 cm^{-1} and 2899 cm^{-1} , which can be attributed to the formation of 1-butene (Fig. 1c,d; spectra after 40 min). There are also (weaker) signatures of the 2-butenes which can be more clearly seen after long reaction times (60 min), when the bands of 1-butene started to vanish and stronger IR bands appeared at 3038 cm^{-1} , 2937 cm^{-1} and 964 cm^{-1} , characteristic of 2-butenes. In addition, peaks appearing at 2966 cm^{-1} and 2881 cm^{-1} are a clear fingerprint of *n*-butane formation. These results agree well with the corresponding GC measurements. At the beginning of the reaction, butadiene is mainly hydrogenated to 1-butene through 1,2-hydrogen addition (Fig. 1c,d; spectra after 40 min), while once 1,3-butadiene has been (nearly) completely consumed, 1-butene is strongly re-adsorbed yielding *n*-butane through hydrogenation and *trans/cis*-2-butene through isomerization (Fig. 1c,d; spectra after 60 min). Compared to the GC measurements, the consumption of 1,3-butadiene is slightly faster in the IRAS experiment due to the smaller volume of the IR cell (although one also has to confess that the 4 products can not always be fully differentiated by IRAS).

Beside catalytic activity and selectivity, deactivation is another important aspect in heterogeneous catalysis. For many hydrocarbon reforming reactions one of the main reasons of deactivation is the dehydrogenation to carbonaceous (CH_x) and C species. In order to quantify the possible effect of carbon deposits on the deactivation of 1,3-butadiene hydrogenation we have performed post-reaction XPS analysis. Using a calibration by adsorbed CO we are able to identify and quantify the carbon species on the surface after the reaction. Fig. 1b shows the C1s and Pd3d signals for the Pd(111) single crystal after 60 min reaction time (after the IRAS measurements). As can be observed, the C1s spectra exhibit a single band centered at 284.2 eV which corresponds to carbon species (CH_x and/or C) adsorbed on the surface together with some remaining butadiene. These carbon species are typically responsible for the deactivation of the catalyst with reaction time. A quantitative analysis of the carbon deposits yielded a carbon coverage of 0.3 ML. Although the amount of carbon formed after 60 min reaction time at 300 K is certainly not negligible,

most of the surface is still clean (especially if carbon forms clusters). This may explain why no significant deactivation was observed in repeated GC measurements. Furthermore, the consecutive 1-butene hydrogenation reaction (Fig. 1a after 75 min reaction time) exhibited an activity similar to that of 1,3-butadiene hydrogenation. Since the hydrogenation rates of both reactions on a clean surface are quite similar this again points to a (nearly) clean surface. The deactivation of the hydrogenation reaction due to carbon deposits must therefore be of minor importance, at least on our timescales. This is somewhat in variance with previous studies on Pd model catalysts where a clear deactivation of the subsequent butene hydrogenation process was observed together with the formation of significant carbon deposits (~ 1 ML) [5]. However, the longer reaction time (6 h) together with the higher reaction temperature (340 K) of these studies [5] probably account for the observed differences. Higher carbon amounts (1–1.5 ML) were previously observed and analyzed during methanol decomposition on Pd(111) at 300 K [19,20]. Interestingly, a flash of the Pd(111) sample above 600 K (not shown) leads to the disappearance of the 284.2 eV band. According to previous studies, this is a clear indication of carbon dissolution (migration) into the Pd bulk at high temperature [20]. Additionally, the absence of any shift in the Pd3d binding energy after reaction (Fig. 1b) rules out the formation of a Pd-carbide (like) phase, such as those reported for acetylene hydrogenation on Pd catalysts at 373 K [21] and for C_2H_4 –Pd(111) interaction [22]. This may again be due to the shorter reaction time and the low reaction temperature used in our study. In summary, post-reaction XPS analysis shows that under the reaction conditions used in our previous investigations on Pd single crystals [12] and Al_2O_3 supported Pd nanoparticles [13] the effect of deactivation by carbon deposits must have been nearly negligible.

The selectivity towards the first hydrogenated products (butenes) is strongly affected by the adsorption strength (stability) of both the reactant and the intermediate reaction products. Previous DFT calculations on butadiene and butene adsorption on Pd(111) suggest that 1,3-butadiene adsorption is ~ 79 $\text{kJ} \cdot \text{mol}^{-1}$ stronger than that of the most strongly adsorbed butene, i.e. 1-butene [16]. This was experimentally confirmed by kinetic analysis of competitive butadiene–butene hydrogenation reactions [9]. Thus, the presence of strongly adsorbed 1,3-butadiene will mostly prevent (or, at least, hinder) the re-adsorption and hydrogenation of butene intermediates to *n*-butane, thereby increasing the selectivity. However, if the adsorption of butadiene is too strong undesired dehydrogenation processes may occur, which produce coke and lead to catalyst deactivation. The interaction of 1,3-butadiene with Pd(111) was therefore studied in more detail by UHV measurements.

3.2. Ultrahigh vacuum measurements

In order to gain more insight into the stability and reactivity of butadiene adsorbed on Pd(111) we have

performed adsorption–desorption XPS measurements under UHV. Fig. 2a shows XPS data acquired during the (multilayer) growth of 1,3-butadiene on Pd(111) at 100 K. At low butadiene exposure (0.5 L; 1 L = 10^{-6} Torr s), the C1s XP spectrum exhibits a broad band centered at 284.0 eV. Increasing the exposure of 1,3-butadiene to 1 L produces a shift in the binding energy to 284.7 eV, together with a low energy tail at \sim 284 eV. A further increase in the butadiene dose up to 20 L produces a symmetric peak centered at 285.1 eV. The increase in the amount of adsorbed butadiene is accompanied by a decrease in the Pd3d intensity (Fig. 2b). However, it is interesting to note that despite of having a butadiene multilayer after 20 L dose, there is still a strong Pd3d signal.

Fig. 2c and d show the quantitative analysis of the XPS data. By using the (2 \times 2)-3 CO saturation structure of CO on Pd(111) for calibration we have quantified the carbon coverage as a function of butadiene exposure (Fig. 2c). Obviously, the carbon coverage increased with butadiene dose. According to these results, exposure of only 1 L butadiene is enough to create a monolayer of carbon on the Pd surface. Taking into account that each butadiene molecule possesses four carbon atoms, this carbon coverage corresponds to a butadiene coverage of 0.25 molecules butadiene/Pd surface atom (we define this as a butadiene

monolayer). An increase in the butadiene dose up to 20 L produced a multilayer corresponding to approximately four layers of butadiene. The formation of a monolayer already after 1 L dose also explains the shift in the C1s binding energy with exposure (Fig. 2d). Below monolayer coverage, the adsorbed butadiene molecules interact directly with the surface and exhibit a lower C1s binding energy (284.0 eV). However, after monolayer formation (1 L), additional butadiene molecules start to adsorb in a multilayer and exhibit a smaller interaction with the surface, leading to a sudden shift to higher binding energies (285.0 eV; this value being constant for further butadiene exposure).

The stability of adsorbed butadiene was addressed by performing temperature-dependent XPS, monitoring the remaining surface species via their C1s and Pd3d signals (Fig. 3a,b, respectively). As observed in the C1s spectra, increasing the sample temperature to 125 K produced a small decrease in intensity, probably due to desorption of weakly bound butadiene from the multilayer (see also Fig. 3c,d). Surprisingly, a further increase in sample temperature up to 500 K led to a binding energy shift to *higher* values, while the peak area (intensity) remained unchanged. Only above 500 K there is a decrease in C1s peak intensity, together with a shift to lower binding energies (Fig. 3c,d).

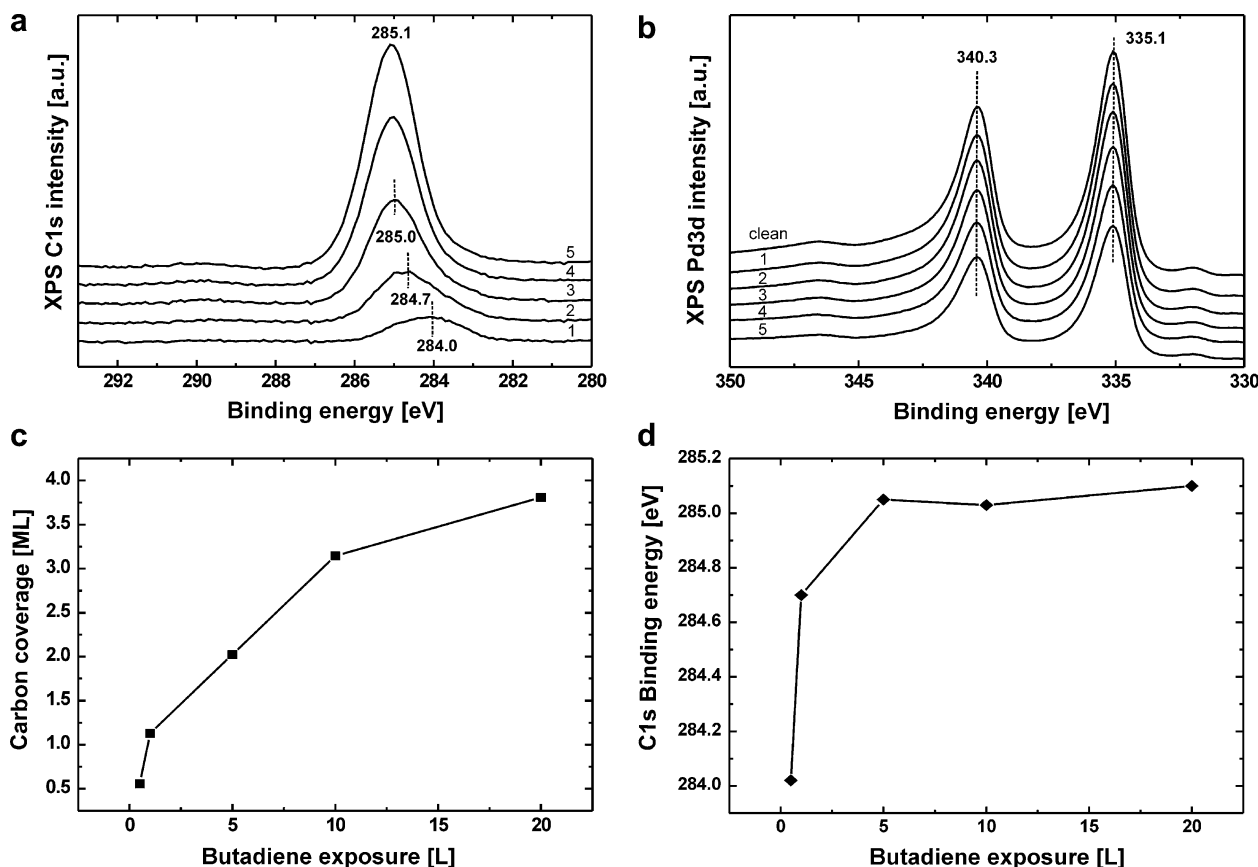


Fig. 2. Photoelectron spectra in the C1s (a) and Pd3d (b) region acquired during butadiene adsorption on Pd(111) at 100 K. Spectra were taken after 0.5 L (trace 1), 1 L (trace 2), 5 L (trace 3), 10 L (trace 4) and 20 L (trace 5) butadiene exposure. XPS analysis of the carbon coverage and C1s binding energy as a function of the butadiene exposure at 100 K are shown in (c) and (d), respectively.

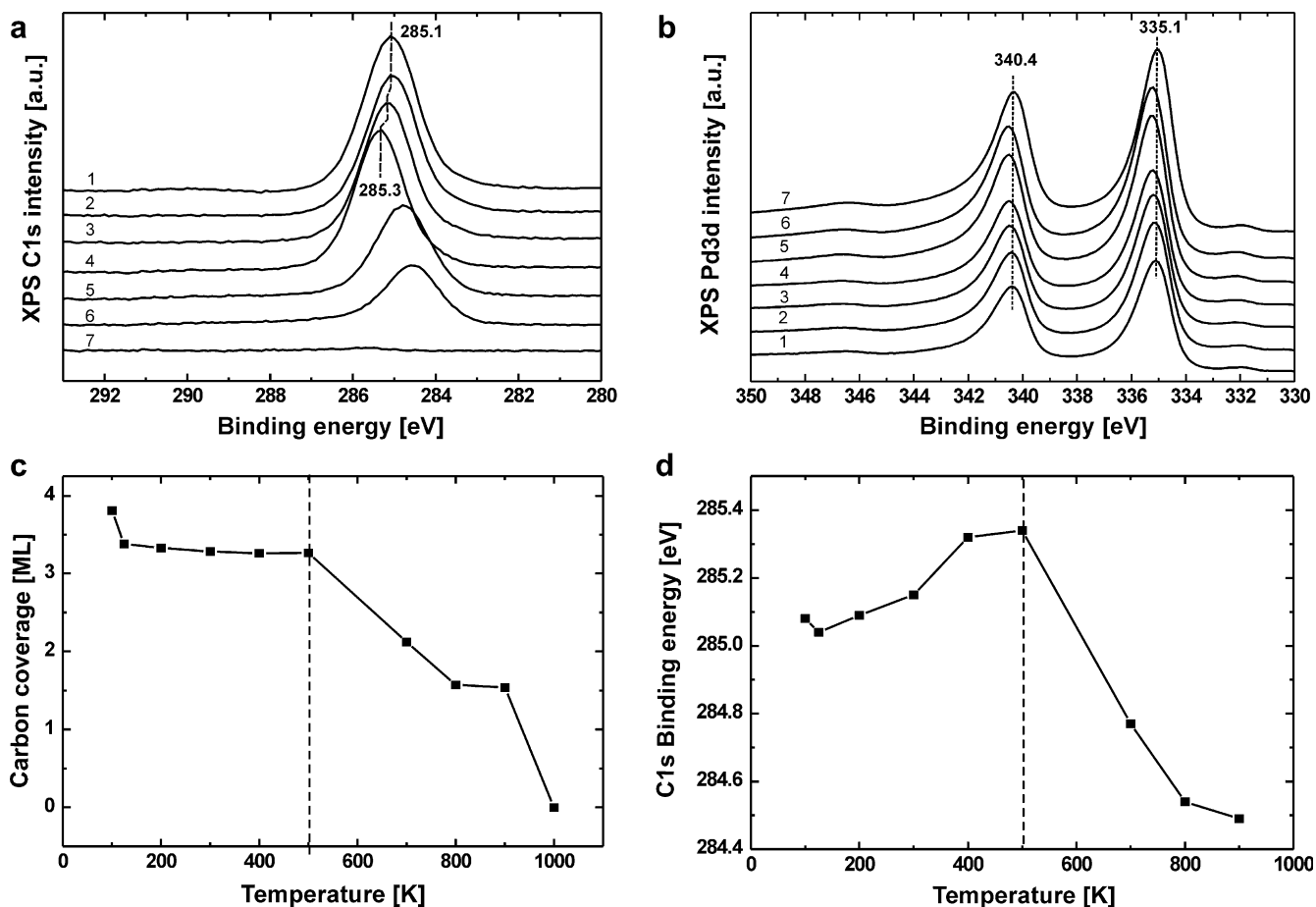


Fig. 3. Photoelectron spectra in the C1s (a) and Pd3d (b) region acquired during annealing a butadiene multilayer on Pd(111). Spectra were taken after 20 L butadiene exposure at 100 K (trace 1), at 125 K (trace 2), at 300 K (trace 3), at 500 K (trace 4), at 700 K (trace 5), at 800 K (trace 6) and at 1000 K (trace 7). XPS analysis of the carbon coverage and C1s binding energy as a function of the annealing temperature are shown in (c) and (d), respectively.

The high stability of adsorbed butadiene towards desorption and decomposition on Pd(111) up to ~500 K is similar to that reported for the same molecule on Pt(111) [10]. Temperature programmed desorption (TPD) spectra after butadiene adsorption on Pt(111) at 100 K showed only desorption of the physisorbed layer but not of chemisorbed butadiene. By following the H₂ signal, very limited butadiene decomposition was observed. The high stability of butadiene adsorbed on close-packed surfaces, i.e. Pd(111) and Pt(111), is a clear evidence of the strong interaction between the diene molecule and the metal surface. A strong adsorption of butadiene on Pd(111) may in fact be responsible for blocking effects on hydrogen adsorption on Pd nanoparticles supported on Al₂O₃, as suggested previously [13].

It is also worth to note the shift in the C1s binding energy between 125 K and 500 K. NEXAFS and HREELS studies of butadiene adsorption on Pd(111) have shown an increase in the bond strength of (di- π bonded) butadiene when the temperature was increased from 95 K to 300 K [7]. The absence of butadiene desorption below 500 K together with the BE shift to *higher* values is a clear indication of a change in the adsorption mode of butadiene with

increasing temperature (while dehydrogenation to carbonaceous deposits (CH_x and/or C) would shift the C1s binding energy to *lower* values (~284.0 eV)). Nevertheless, the occurrence of initial steps of dehydrogenation, e.g. butadiene dehydrogenation to butylidyne, can not be fully ruled out. Previous studies of ethylene adsorption on Pd(111) and Pt(111) have shown that while ethylene is dehydrogenated to ethylidyne on Pt(111), the molecule rather desorbed from Pd(111) upon annealing to 300 K, without conversion or decomposition to other species [14,23]. According to Fig. 3, butadiene decomposes above 500 K, most likely through dehydrogenation producing CH_x and C species on the surface, as indicated by the shift of the C1s signal to lower binding energies (284.0 eV), values typical of carbon and hydrocarbon species [20,24]. The decreasing intensity indicates carbon dissolution and at 1000 K the C1s signal fully disappeared, due to carbon migration into the Pd bulk (Fig. 3c).

The Pd3d spectra revealed a small (~+0.2 eV) shift between ~500 K and 800 K (Fig. 3b), while at lower and higher temperature peak positions typical of metallic Pd were observed. This temperature dependence is probably an indication that upon butadiene decomposition (and

simultaneous carbon dissolution) above 500 K a carbide-like Pd_xC_y phase is formed (between 500 K and 800 K [22,25,26]), but its exact nature is currently unknown. This intermediate Pd_xC_y phase decomposed at higher temperature and at 1000 K the Pd3d signal shifted back to 335.1 eV (metallic Pd), because carbon dissolved deep in the Pd volume.

4. Conclusion

Ambient pressure kinetic studies of selective 1,3-butadiene hydrogenation on Pd(111) at 300 K identified 1-butene, *trans*-2-butene and *cis*-2-butene as primary products. Contrary to the behavior on Pd nanoparticles [13], the Pd(111) single crystal exhibits a lower selectivity towards butene formation, with *n*-butane formed already in the first minutes of the reaction. The hydrogenation process is accompanied by re-adsorption of butenes, i.e. mainly 1-butene, producing *n*-butane through hydrogenation and *trans/cis*-2-butene through isomerization. With decreasing 1-butene concentration, hydrogenation of 2-butenes sets in. This was corroborated by IRAS experiments which monitored the gas phase species (while no surface species could be observed). Post-reaction XPS studies detected ~0.3 ML carbon species on the surface, i.e. adsorbed butadiene and/or carbon deposits. Thus, deactivation due to coking was only a minor effect under our reaction conditions.

Temperature-dependent XPS experiments under UHV showed that butadiene is highly stable towards desorption and/or decomposition on the Pd(111) surface up to ~500 K. This strong interaction of the diene molecule with the Pd surface must be responsible for the blocking effects on hydrogen adsorption and butene re-adsorption, as reported previously for Pd nanoparticles supported on Al_2O_3 [13]. However, care must still be taken when comparing UHV results with the atmospheric pressure kinetic studies, due to the pressure difference and due to the absence of hydrogen in the UHV measurements (very likely, adsorbed H would modify the diene adsorption properties). A high temperature treatment of the butadiene covered Pd(111) surface indicated decomposition processes (dehydrogenation) and (partial) carbon dissolution into the Pd bulk. Similar spectroscopic studies on supported Pd nanoparticles are planned for the future.

Acknowledgements

J.S.A. acknowledges the support by the Alexander von Humboldt Foundation. M.B. is grateful for a fellowship by the International Max Planck Research School. This

work was partly supported by the German Science Foundation (SPP 1091; Project Ru 831/1-4).

References

- [1] F.H. Puls, K.D. Ruhnke, Butene-1 containing feed purification process (CS-165), US Patent, No. 4260840, 1980.
- [2] H.U. Hammershaimb, J.B. Spinner, HF alkylation and selective hydrogenation process, US Patent, No. 4774375, 1988.
- [3] K. Flick, C. Herion, H.M. Allmann, Supported palladium catalyst for selective catalytic hydrogenation of acetylene in hydrocarbonaceous streams, US Patent, No. 5856262, 1999.
- [4] H. Arnold, F. Dölbart, J. Gaube, Handbook of Heterogeneous Catalysis, in: G. Ertl, H. Knözinger, J. Weitkamp (Eds.), Wiley-VCH, 1997, vol. 3, p. 2165.
- [5] J. Massardier, J.C. Bertolini, A. Renouprez, in: Proceedings of the 9th International Congress on Catalysis, Calgary, 1988, p. 1222.
- [6] J.C. Bertolini, A. Cassuto, Y. Jugnet, J. Massardier, B. Tardy, G. Tourillon, Surf. Sci. 349 (1996) 88.
- [7] G. Tourillon, A. Cassuto, Y. Jugnet, J. Massardier, J.C. Bertolini, J. Chem. Soc., Faraday Trans. 92 (1996) 4835.
- [8] K. Christmann, G. Ertl, T. Pignet, Surf. Sci. 54 (1976) 365.
- [9] T. Ouchaib, J. Massardier, A. Renouprez, J. Catal. 119 (1989) 517.
- [10] H. Zhao, B.E. Koel, Surf. Sci. 572 (2004) 261.
- [11] S. Katano, H.S. Kato, M. Kawai, K. Domen, J. Phys. Chem. B 107 (2003) 3671.
- [12] J. Silvestre-Albero, G. Rupprechter, H.J. Freund, J. Catal. 235 (2005) 52.
- [13] (a) J. Silvestre-Albero, G. Rupprechter, H.J. Freund, Chem. Commun. (2006) 80; (b) J. Silvestre-Albero, G. Rupprechter, H.-J. Freund, J. Catal. 240 (2006) 58.
- [14] (a) G. Rupprechter, Annu. Rep. Prog. Chem. Sect. C 100 (2004) 237; (b) M. Morkel, G. Rupprechter, H.-J. Freund, J. Chem. Phys. 119 (2003) 10853.
- [15] (a) J.J. Phillipson, P.B. Wells, G.R. Wilson, J. Chem. Soc. A 9 (1969) 1351; (b) A.J. Bates, Z.K. Leszczynski, J.J. Phillipson, P.B. Wells, G.R. Wilson, J. Chem. Soc. A 14 (1970) 2435.
- [16] A. Valcarcel, A. Clotet, J.M. Ricart, F. Delbecq, P. Sautet, Surf. Sci. 549 (2004) 121.
- [17] Y. Jugnet, R. Sedrati, J.C. Bertolini, J. Catal. 229 (2005) 252.
- [18] S. Katano, S. Ichihara, H. Ogasawara, H.S. Kato, T. Komeda, M. Kawai, K. Domen, Surf. Sci. 502–503 (2002) 164.
- [19] M. Morkel, V.V. Kaichev, G. Rupprechter, H.-J. Freund, I.P. Prosvirin, V.I. Bukhtiyarov, J. Phys. Chem. B 108 (2004) 12955.
- [20] O. Rodriguez de la Fuente, M. Borasio, P. Galletto, G. Rupprechter, H.J. Freund, Surf. Sci. 566–568 (2004) 740.
- [21] J. Stachurski, A. Frackiewicz, J. Less-Common Met. 108 (1985) 249.
- [22] H. Gabasch, K. Hayek, B. Klötzer, A. Knop-Gericke, R. Schögl, J. Phys. Chem. B 110 (2006) 4947.
- [23] L.P. Wang, W.T. Tysoe, R.M. Ormerod, R.M. Lambert, H. Hoffmann, F. Zaera, J. Phys. Chem. 94 (1990) 4236.
- [24] M. Borasio, O. Rodriguez de la Fuente, G. Rupprechter, H.J. Freund, J. Phys. Chem. B 109 (2005) 17791.
- [25] D. Teschner, A. Pestryakov, E. Kleimenov, M. Hävecker, H. Bluhm, H. Sauer, A. Knop-Gericke, R. Schlögl, J. Catal. 230 (2005) 186.
- [26] D. Teschner, A. Pestryakov, E. Kleimenov, M. Hävecker, H. Bluhm, H. Sauer, A. Knop-Gericke, R. Schlögl, J. Catal. 230 (2005) 195.